

## ADVANCES IN THE MODELING AND CONTROL OF BATCH CRYSTALLIZERS

Zoltan K. Nagy, Jia W. Chew, Mitsuko Fujiwara, Richard D. Braatz

*University of Illinois at Urbana-Champaign  
Department of Chemical and Biomolecular Engineering  
600 South Mathews Avenue, Urbana, IL 61801*

**Abstract:** Despite the widespread application of crystallization, there are still a disproportionate number of problems associated with its control. These problems have become important in recent years as increased interest has been directed towards the crystallization of pharmaceuticals and proteins, which have additional complications compared to the inorganic crystallizations studied extensively in the past 50+ years. This paper covers recent advances in batch crystallization modeling and control. This includes a comparison in simulations and experiments between the classical temperature control approach developed in the 1970-90s with new concentration control approach developed in the last few years. The new approach, which uses ATR-FTIR spectroscopy and feedback control to follow a setpoint trajectory in the solution concentration as a function of temperature, results in reduced sensitivity of the product quality to disturbances. The resulting guidelines from the simulations are applied to the crystallization of paracetamol in water. *Copyright © 2003 IFAC*

**Keywords:** particulate processing, batch control, particle size measurement, uncertain dynamic systems, parameter estimation, nonlinear systems, spectroscopy, distributions, modelling errors, optimal control

### 1. INTRODUCTION

Despite the long history and widespread application of batch crystallization, there are a disproportionate number of problems associated with its control. These problems have become especially important in recent years as an increased interest has been directed towards the crystallization of pharmaceuticals and proteins, which have additional complications compared to the inorganic batch and continuous crystallizations studied extensively over the past 50+ years. Many problems in downstream processes can be attributed to poor particle characteristics established in the crystallization step. The control objectives for batch crystallization processes can be defined in terms of product purity, crystal habit, morphology, average particle size, crystal size distribution, bulk density, product filterability, and dry solid flow properties. Recent advances in sensor

technology have brought on-line feedback control within the realm of possibility (Braatz, 2002). On-line control during batch crystallization offers the possibilities for improved crystal product quality, shorter process times, and reduction or elimination of compromised batches.

The fundamental driving force for crystallization from solution is the difference in the chemical potential; however, it is more convenient to write the driving force in terms of the supersaturation, which is the difference between the solution concentration and the saturation concentration. The size, shape, and solid-state phase of the product crystals are dependent on the supersaturation profile achieved during the crystallization process. Supersaturation is usually created by cooling, evaporation, or solvent addition. For brevity, this review will primarily discuss cooling crystallization, although the

principles apply to other methods of supersaturation creation.

Most past studies in batch crystallization control have dealt with finding the open-loop temperature versus time trajectory that optimizes some characteristics of the desired crystal size distribution, as discussed in several review papers (Braatz, 2002; Rawlings *et al.*, 1993). This classical approach requires the development of a first-principles model with accurate growth and nucleation kinetics, which can be obtained in a series of continuous or batch experiments. Uncertainties in the parameter estimates, nonidealities in the model assumptions, and disturbances have to be taken into account to ensure that this approach results in the expected optimized product quality (Eaton and Rawlings, 1990; Ma and Braatz, 2003; Ma *et al.*, 1999; Srinivasan *et al.*, 2003; Terwiesc *et al.*, 1994).

A new alternative *direct design* approach to controlling a batch crystallizer is based on the understanding that the desired region of operation for most crystallizers is within the metastable zone (see Figure 1), which is bounded by the solubility curve and the metastable limit (Mullin, 1993). This approach uses a feedback control system to follow a solution concentration trajectory as a function of temperature (Feng and Berglund, 2002; Fujiwara *et al.*, 2002; Gutwald and Mersmann, 1990; Grön *et al.*, 2003), where this setpoint trajectory is designed to lie within the metastable zone. The setpoint supersaturation curve is the result of the compromise between the desire for a fast crystal growth rate that occurs near the metastable limit, and a low nucleation rate, which takes place near the solubility curve. The advantage of this approach is that, unlike the first approach, it does not require the derivation of accurate growth and nucleation kinetics. Hence, it can be easily implemented based on the automated determination of the solubility curve and the metastable limit (Barrett and Glennon, 2002; Fujiwara *et al.*, 2002).

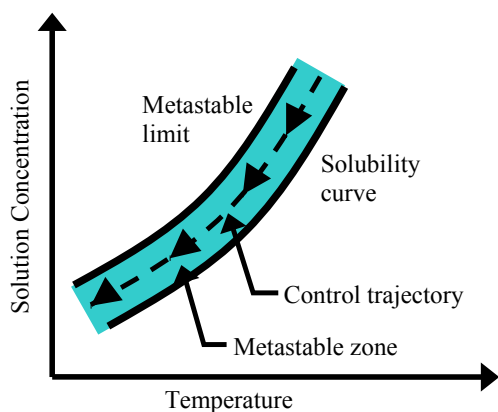


Fig. 1. The metastable zone, solubility curve, metastable limit, and concentration-temperature control trajectory. Similar notions apply to antisolvent and evaporative crystallization.

This paper uses a combination of simulations and experiments to describe and compare the classical temperature control approach with the direct design approach. This assessment considers the effects of parameter uncertainties and disturbances for the crystallization of an important pharmaceutical, paracetamol (acetaminophen). A wide variety of disturbance scenarios (e.g., shifts in the solubility curve, deviations in seeding, evaporation) are investigated. The advantages and disadvantages of each control approach are discussed. Understanding these tradeoffs provides guidance as to the best control strategy for a particular crystallization process.

## 2. BATCH CRYSTALLIZATION OPERATIONS

Usually the main objective of batch crystallization is to produce large uniform crystals within a given time. Since a large number of nuclei forms if the supersaturation crosses the metastable limit, most crystallizers are operated by adding seeds near the start of the batch and maintaining the supersaturation within the metastable zone, where the nucleation and growth processes compete for the solute molecules. Both the nucleation and growth rates are positively correlated with supersaturation. An optimal control strategy should have a high enough supersaturation that the growth rate is significant (so that the batch runs are not too long) but low enough supersaturation to keep the rate of nucleation low. Seeding reduces the productivity of each batch, but can lead to more consistent crystals when the crystallizer is poorly controlled. An alternative unseeded method creates the seed inside the crystallizer. Figure 2 shows typical operating lines for each method, in the concentration versus temperature diagram. For seeded operation the seed is introduced shortly after the solubility curve is crossed and the operating line should remain within the metastable zone. For unseeded operation the operating line first reaches the metastable limit to generate a controlled nucleation and then the supersaturation should be kept below the metastable limit similar to the seeded system.

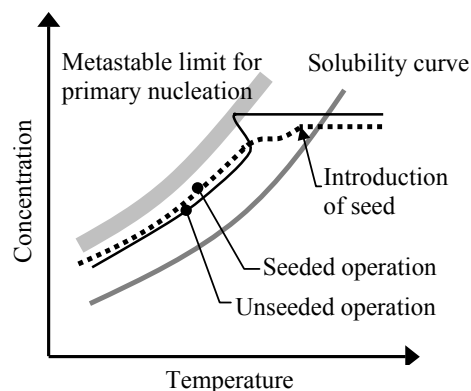


Fig. 2. Concept of seeded and unseeded batch cooling crystallization.

### 3. MODEL IDENTIFICATION

This section describes how parameters are estimated in batch crystallization. Because the most popular parameter estimation algorithms iteratively call the simulation model, the method of moments is usually used to reduce the simulation time. The  $j$ th moment when there is one characteristic size dimension is

$$\mu_j = \int_0^{\infty} L^j f(L, t) dL, \quad (1)$$

where  $f(L, t)$  is the crystal size distribution,  $L$  is the crystal size, and  $t$  is time. Typically the four lowest order moments are simulated since many properties of the crystal size distribution (CSD) can be expressed as a function of these moments. After some simplifying assumptions (Miller and Rawlings, 1994), the model equations are:

$$\begin{bmatrix} \dot{\mu}_0 \\ \dot{\mu}_1 \\ \dot{\mu}_2 \\ \dot{\mu}_3 \\ \dot{C} \end{bmatrix} = \begin{bmatrix} B \\ G\mu_0 + Br_0 \\ 2G\mu_1 + Br_0^2 \\ 3G\mu_2 + Br_0^3 \\ -\rho_c k_v (3G\mu_2 + Br_0^3) \end{bmatrix}, \quad (2)$$

where  $C$  is the solution concentration expressed in mass of crystal per unit mass of solvent,  $r_0$  is the crystal size at nucleation,  $\rho_c$  is the density of the crystal, and  $B$  and  $G$  are the nucleation and growth rates, respectively. The growth kinetics are typically assumed to satisfy

$$G = k_g \Delta C^g. \quad (3)$$

The solubility is a function of temperature. For the paracetamol crystals used here as a demonstrative system, the experimentally determined solubility curve is (Fujiwara *et al.*, 2002)

$$C^*(T) = 1.5846 \cdot 10^{-5} T^2 - 9.0567 \cdot 10^{-3} T + 1.3066. \quad (4)$$

For the modeling performed here, the crystallizer is unseeded, so that the classical and direct design approaches are compared for the more challenging control problem. Then the unseeded nucleation rate is given by

$$B = k_b \Delta C^b, \quad (5)$$

which is referred to as ‘‘primary nucleation’’ in the literature (Mullin, 1993). The initial condition for (2) is given by  $\mu_i(0) = 0$  ( $i = 0, 1, 2, 3$ ), and  $C(0) = C_i$ . The crystal size at nucleation is considered very small ( $r_0 \approx 0$ ).

**Table 1. Kinetic parameters for the unseeded crystallization of paracetamol in water, estimated from data collected during the determination of the metastable limit for primary nucleation**

$B$	$\ln(k_b)$	$g$	$\ln(k_g)$
$6.2 \pm 0.9$	$45.8 \pm 4.6$	$1.5 \pm 0.5$	$4.1 \pm 1.2$

Kinetic parameter estimation and control experiments were performed using pharmaceutical grade paracetamol (4-aminodiphenol, 98% purity, obtained from Aldrich) in a 500 ml jacketed round bottom flask with an overhead stirrer. Degassed deionized water was used to prepare the solutions. During the experiments the solution concentration was measured using ATR-FTIR spectroscopy coupled with robust chemometrics (Togkalidou *et al.*, 2001; Fujiwara *et al.*, 2002). In this procedure aqueous paracetamol spectra were obtained using a DIPPER-210 ATR immersion probe (Axiom Analytical) with two reflections with a ZnSe internal reflectance element. The probe was attached to a Nicolet Protege 460 FTIR spectrophotometer connected to a desktop PC running OMNIC 4.1a software from Nicolet Instrument Corp. The spectrometer was purged with N<sub>2</sub> gas 1.5 hours before and while measurements were being taken to reduce the effects of CO<sub>2</sub> absorption in its optical path. Each output of FTIR spectra were averaged over 32 scans (which took ~20 s) with a spectral resolution of 4 cm<sup>-1</sup>. The obtained IR spectra were used to estimate the solution concentration based on the calibration model. Chord length distributions of paracetamol crystals in solution were obtained using Lasentec Focused Beam Reflectance Measurement (FBRM) connected to a Pentium III running version 6.0b9 of the FBRM Control Interface software. FBRM collects backscattered light from a focused laser beam emitted from the probe tip, with the chord length distribution based on the measured particle size measured by the laser beam (Braatz, 2002). Geometric inverse modeling (Hukkanen and Braatz, 2002) was used to compute the particle size distribution from the chord length distribution, and the moment ratios  $\mu_1/\mu_0$ ,  $\mu_2/\mu_0$ , and  $\mu_3/\mu_0$  were computed using a high order discretization of the integral (1). These ratios, which are the mean crystal size, area, and volume, normalize out sampling effects that occur as the solids density increases. Ratios of the larger moments are not used due to their sensitivity to the sampling of large particles (Gunawan *et al.*, 2002). The sample temperature was controlled by ratioing the hot and cold water to the jacket with a research control valve (Badger Meter, Inc.) using a proportional-integral control system designed via internal model control. The crystallizer temperature was measured every 2 seconds using a Teflon-coated thermocouple attached to a Data Translation 3004 data acquisition board via a Fluke 80TK thermocouple module. The same instrument conditions were used for all experiments.

The measured solution concentration  $C$  and moment ratios  $\mu_1/\mu_0$ ,  $\mu_2/\mu_0$ , and  $\mu_3/\mu_0$  for a series of metastable limit experiments were used to compute maximum likelihood estimates of the four kinetic parameters ( $k_b$ ,  $b$ ,  $k_g$ ,  $g$ ). The nonlinear optimization was solved using successive quadratic programming. The details of the experimental and parameter estimation procedures are available elsewhere (Nagy *et al.*, 2002). The resulting kinetic parameters with their confidence intervals are given in Table 1.

#### 4. CONTROL STRATEGIES

The temperature control approach is the simplest and most widely used technique. The only measurement required is the temperature in the crystallizer (and jacket if cascade control is used). Figure 3 is a schematic diagram of this approach. The controller tracks a setpoint temperature profile in time by manipulating the jacket temperature (via modifying the cooling water flow rate or the ratio between cold and hot water flow rates). The setpoint temperature profile may be obtained using trial-and-error, or open-loop or closed-loop optimal control if an accurate dynamic model is available. In open-loop optimal control, the setpoint temperature profile is usually parameterized by a linear piecewise function, with the temperatures at the sampling instances being the optimization variables. Various CSD properties have been used as the objective function with the most common being to maximize the mean crystal size

$$L_n = \frac{\mu_1}{\mu_0}. \quad (6)$$

The optimal control problem is then:

$$\min_{T(1), T(2), \dots, T(N)} L_n \quad (7)$$

subject to the constraints of the model equations (2) and

$$\begin{aligned} T_{min} &\leq T(k) \leq T_{max}, \\ R_{min} &\leq dT/dt \leq R_{max}, \\ C_{final} &\leq C_{final, max}. \end{aligned}$$

where  $T_{min}$ ,  $T_{max}$ ,  $R_{min}$ , and  $R_{max}$  are the minimum and maximum temperatures and temperature ramp rates, respectively, during the batch. The first two inequality constraints ensure that the temperature profile can be implemented. The last inequality constraint ensures that the minimum yield is achieved as specified by economic considerations. The successive quadratic programming solution of the optimal control problem (7) gives the temperature trajectory in Figure 4. The initial temperature drop creates nuclei by a controlled primary nucleation. The optimum temperature trajectory ensures that, after the required number of seeds is created, the nucleation rate drops off rapidly (see Figure 5). Note that the growth rate corresponding to the optimum temperature profile is nearly constant after the initial seed generation step of the process, leading to a nearly linear increase in the mean size  $L_n$  (see Figure 4) with the maximum theoretical value at the end of the batch equal to 109  $\mu\text{m}$ , with a yield of 44%.

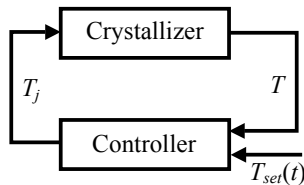


Fig. 3. Schematic block diagram of the classical temperature control approach.

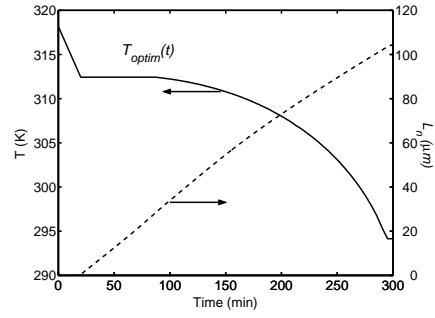


Fig. 4. Simulated optimum temperature profile and change in mean crystal size for the crystallization of paracetamol in water.

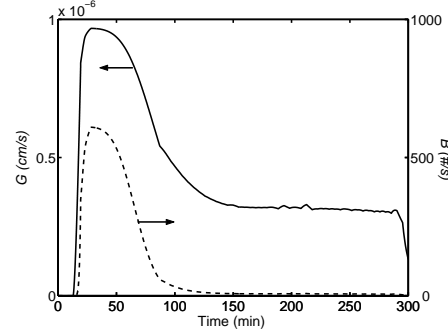


Fig. 5. Variation of the growth rate and nucleation rate corresponding to the optimum temperature profile for simulated unseeded crystallization of paracetamol in water.

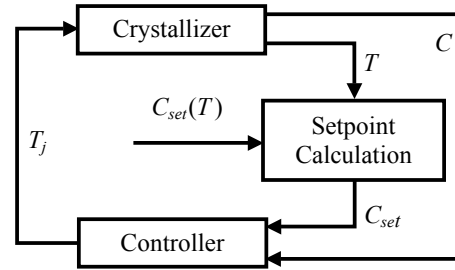


Fig. 6. Schematic block diagram of the concentration versus temperature control approach.

The classical approach requires rather accurate model parameters, or the benefits of optimal control may be lost. Although some uncertainty in the kinetic parameters may be handled through robust feedback control systems (Nagy and Braatz, 2002), there will always be model structure errors (e.g., nonideal mixing) that are not captured by the uncertainty description. This is partly why the most common method used in industry to design the setpoint temperature profile is by trial-and-error experiments.

The direct design approach shown in Figure 6 follows a setpoint concentration versus temperature profile within the metastable zone. This approach does not require a detailed model or kinetic parameters of the process. A close-to-optimal concentration versus temperature setpoint can be obtained based on experimental determination of the

solubility curve and metastable limit (Barrett and Glennon, 2002; Fujiwara et al., 2002; Lewiner et al., 2001), procedures that can be easily automated. Besides the temperature measurement, this approach requires solution concentration measurements, which can be collected using ATR-FTIR spectroscopy, which can produce concentration measurements within 0.01wt%. The  $C_{set}(T)$  trajectory corresponding to the optimum temperature profile from Figure 4 is shown in Figure 7. The optimum temperature profile creates a higher supersaturation at the beginning to generate the initial nuclei, then it keeps the supersaturation at a nearly constant value within the metastable zone for the rest of the batch.

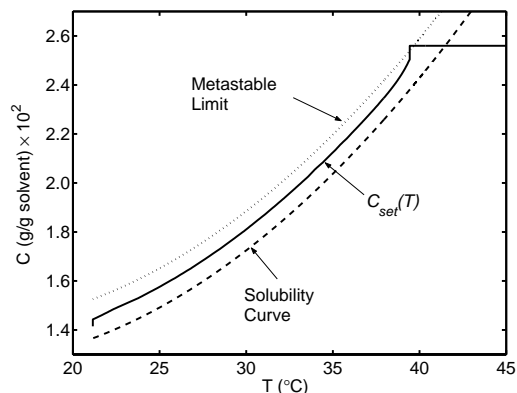


Fig. 7. Setpoint temperature for the concentration control approach.

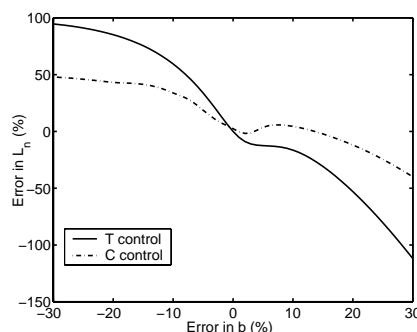


Fig. 8. Sensitivity of the mean crystal size to variation in the nucleation exponent  $b$  for the two control strategies.

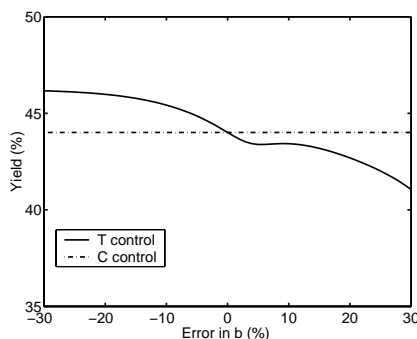


Fig. 9. Sensitivity of the crystallizer yield to variation in the nucleation exponent  $b$  for the two control strategies.

Although the classical T-control and the direct design C-control approaches give identical results under ideal conditions, their sensitivities to disturbances are very different. The effect of variation in the nucleation exponent on the mean size and the yield is shown in Figures 8 and 9. The mean size at the end of the batch is much more sensitive to variation in the nucleation exponent  $b$  for the classical T-control strategy. In addition, the C-control approach leads to constant yield. Unlike T-control where the optimum temperature versus time profile fixes the batch time, in C-control the setpoint is a function of temperature only, leading to variable batch time. Similar trends are obtained for variation in the other kinetic parameters.

Shifts in the solubility curve typically occur in practice due to the presence of inorganic salts or other contaminants in the feedstocks. Evaporation can also occur. The effects of these disturbances are shown in Table 2. An increase or decrease of 5% in the solubility results in significant decrease in the mean size. Both control strategies are highly sensitive to shifts in the solubility curve, with T-control being more sensitive. When a linear decrease of the mass of solvent is simulated (e.g., due to evaporation), the C-control approach is much less sensitive than T-control. The concentration measurement in C-control enables the supersaturation to be maintained when solvent is evaporated. The subsequent experimental results confirm and extend the simulation results.

Table 2. Sensitivity of C- and T- control to disturbances

Disturbance	Decrease in mean size $L_n$ (%)	
	T-control	C-control
Shift in solubility curve	-5%	60
	+5%	53
Variation in mass of solvent	-5%	7
	-10%	11

## 5. EXPERIMENTAL COMPARISON

Figures 10 and 11 show the crystals produced by T-control and C-control where the apparatus was designed to operate with as few disturbances as possible. To make a direct comparison, the setpoint  $C_{set}(T)$  profile used in C-control corresponded to the  $T_{set}(t)$  trajectory used in T-control (see Figure 4). Crystals produced under conditions of minimal disturbances had the same shape, with a somewhat narrower size distribution and less agglomeration for C-control. Even when operating under an artificially low amount of disturbances in the bench-scale experiments, the small disturbances were enough to cause C-control to give a slower average cooling rate, which resulted in the differences in product crystals achieved by the two control strategies.

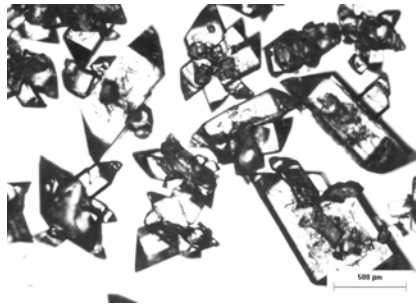


Fig. 10. Microscopy image of paracetamol product crystals for the unseeded system using T-control.



Fig. 11. Microscopy image of paracetamol product crystals for the unseeded system using C-control.

The difference in product quality between the two strategies will be much larger at the manufacturing scale, where the disturbances are much more significant. Consider the disturbance where some seed from a previous batch is not completely dissolved before starting the next batch. Figures 12 and 13 show images of the product crystals for T-control and C-control, respectively, when some seed was left in the batch. The setpoint trajectory  $C_{set}(T)$  was specified to give constant supersaturation after a short period where the temperature is dropped to get to the starting point for the setpoint trajectory. The crystals are much larger and uniform in size and shape for C-control than for T-control. C-control gave high crystal product quality even for this rather large disturbance.

This sensitivity of the product quality to seeds for T-control can be understood by inspection of the concentration-temperature diagram in Figure 14 and the FBRM data in Figure 15. The temperature setpoint caused the solution concentration to cross the metastable limit, as expected, but the presence of seed resulted in lower nucleation (see Figure 15) at 38°C than in unseeded operations. This is consistent with nucleation theory, which predicts that the nucleation rate for seeded operations is much lower than for unseeded operations at high supersaturation (Kim and Mersmann, 2001; Mullin, 1993). Hence most of the reduction in supersaturation at 38°C was due to growth onto the seed crystals rather than the creation of nuclei. The reduced availability of crystal area for growth (less small crystals means less surface area) caused the supersaturation to drift too far from the solubility curve as the temperature was

reduced, crossing the metastable limit and inducing nucleation near the end of the batch run (see Figure 15). Although a specific crystal-solvent system was selected to illustrate the key points, the general physical principles apply. Temperature control of an unseeded crystallizer will give very poor CSD if some seed is accidentally left behind from a previous batch. In a general sense these experimental results are consistent with the simulation results, which indicated the high sensitivity of T-control to variation in the nucleation kinetics.

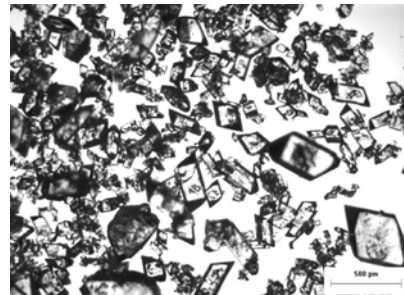


Fig. 12. Microscopy image of paracetamol product crystals for the seeded system using T-control with the setpoint obtained from the optimization of the model of the unseeded system.



Fig. 13. Microscopy image of paracetamol product crystals for the seeded system using C-control.

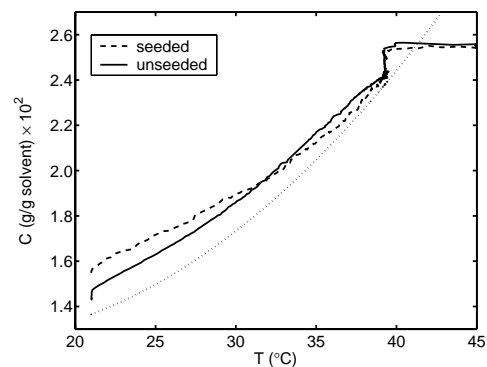


Fig. 14. Concentration-temperature profile of the unseeded and seeded systems operated by T-control.

The insensitivity of C-control to the seeding can be understood from the concentration-temperature diagram in Figure 16 and the FBRM data in Figure 17. The constant value for the supersaturation completely avoided nucleation during the batch. Using feedback control to achieve constant supersaturation, without

optimizing the setpoint trajectory or seeding, gave much higher quality crystals than the optimized classical T-control strategy studied heavily in the literature.

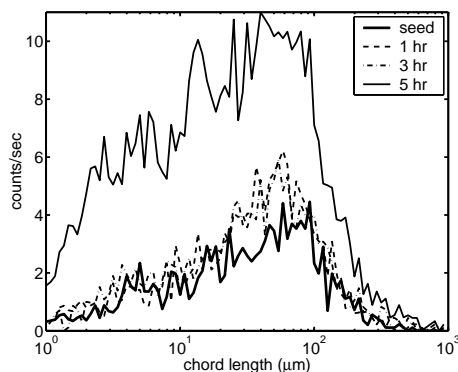


Fig. 15. FBRM chord length distributions at different times during the batch for the T-controlled seeded system.

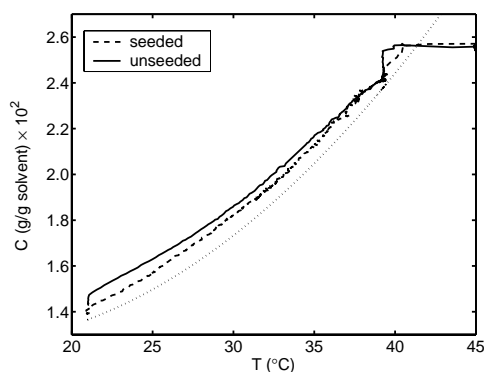


Fig. 16. C-control of seeded and unseeded systems. The seeded system was controlled at a constant supersturation.

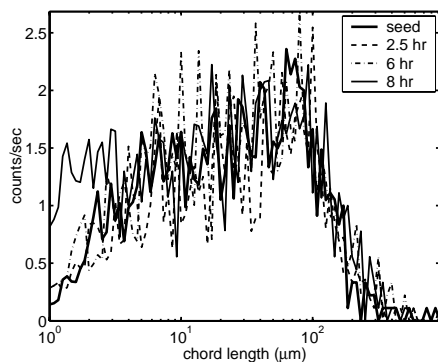


Fig. 17. FBRM chord length distributions at different times during the batch for the C-controlled seeded system.

Although the simulation results indicated that C-control was less sensitive than the classical T-control strategy for most disturbances, recall that both control strategies were sensitive to a shift in the solubility curve. It is well recognized that the presence of small amount of certain impurities can have substantial effects on the crystallization process.

Impurities can suppress primary nucleation, modify solubility, and/or inhibit or enhance the overall growth rate. Certain impurities have a selective effect on the growth rate of the crystallographic surfaces, thus modifying the crystal shape (Mullin, 1993). The effects of additives on the C-control of paracetamol-water crystallization were investigated by introducing 4 mol% acetanilide (AA) to the initial batch. Acetanilide is a structurally related impurity for which moderate primary nucleation inhibition and crystal habit modification effects are reported (Hendriksen *et al.*, 2001). AA also has peaks at similar frequencies of the infrared spectra as paracetamol, thus influencing the solution concentration measurements. The C-control approach was used to conduct the experiment at the same supersaturation as in the case of the seeded system with C-control (with no additive). The FBRM measurements indicated significant nucleation (see Figure 18) leading to the product shown in Figure 19 with poor CSD and small mean size. This indicates that the effect of additive on the solubility and on the concentration measurement was more significant than its nucleation inhibition effect. These experimental results are in accordance with the simulations, which indicated a significant decrease in the mean size when a shift in solubility occurs. The only way to design control systems to suppress the effects of shifts in the solubility is to include direct measurements of the supersaturation or to include measurements of the particle size distribution directly in the control system.

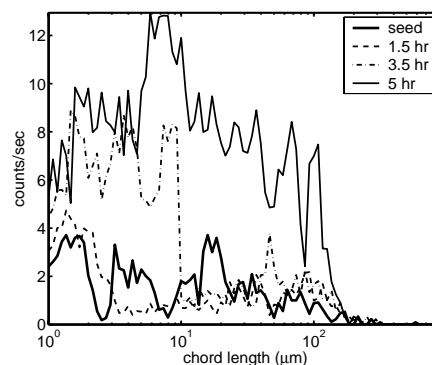


Fig. 18. FBRM chord length distributions at different times during the batch for the C-controlled seeded system with 4% acetanilide additive.

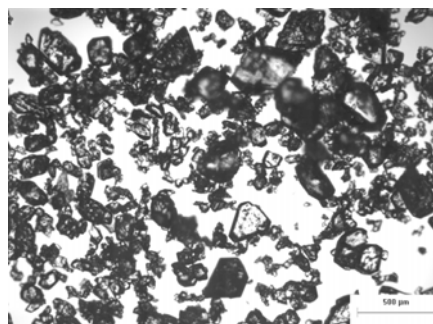


Fig. 19. Microscopy image of paracetamol product crystals for the seeded system using C-control and 4 mol% Acetanilide as additive.

## 5. CONCLUSIONS

This paper reviewed the two main modeling and control approaches for the control of batch crystallizers. The temperature control approach is the tradition in batch cooling crystallization. Unless trial-and-error is used to obtain the setpoint profile, an accurate model is required for computing the optimal control trajectory. The direct design approach controls the solution concentration as a function of temperature, so that a desired supersaturation is controlled within the metastable zone. Simulation and experiments indicated that temperature control is highly sensitive to variation in the kinetic parameters and seeding. In contrast, direct design of the concentration-control system requires no information about the model or kinetic parameters of the process, and is instead based on the automated determination of the metastable zone. Concentration control resulted in lower sensitivity to disturbances than temperature control in almost all cases simulated or tested experimentally. Both control approaches are sensitive to variations in the solubility curve. Also, C-control requires a concentration measurement, so the presence of structurally related contaminating chemicals can degrade the performance of this approach.

## 6. ACKNOWLEDGEMENTS

This work was supported by NSF Award #0108053 and the Merck Research Laboratories.

## REFERENCES

- Barrett, P., and B. Glennon (2002). Characterizing the metastable zone and solubility curve using Lasentec FBRM and PVM. *Chem. Eng. Res. Des.*, **80**, 799-805.
- Braatz, R.D. (2002). Advanced control of crystallization processes. *Annual Reviews in Control*, **26**, 87-99.
- Eaton, J.W., and J.B. Rawlings (1990). Feedback control of chemical processes using on-line optimization techniques. *Comp. & Chem. Eng.*, **14**, 469-479.
- Feng, L.L., and K.A. Berglund (2002). ATR-FTIR for determining optimal cooling curves for batch crystallization of succinic acid, *Crystal Growth & Design*, **2**, 449-452.
- Fujiwara, M., P.S. Chow, D.L. Ma, and R.D. Braatz (2002). Paracetamol crystallization using laser backscattering and ATR-FTIR spectroscopy: Metastability, agglomeration, and control. *Crystal Growth & Design*, **2**, 363-370.
- Grön, H., A. Borrisova, and K.J. Roberts (2003). In-process ATR-FTIR spectroscopy for closed-loop supersaturation control of a batch crystallizer producing monosodium glutamate crystals of defined size. *Ind. Eng. Chem. Res.*, **42**, 198-206.
- Gunawan, R., D.L. Ma, M. Fujiwara, and R.D. Braatz (2002). Identification of kinetic parameters in a multidimensional crystallization process. *Int. J. Modern Physics B*, **16**, 367-374.
- Gutwald, T., and A. Mersmann (1990). Batch cooling crystallization at constant supersaturation. Technique and experimental results. *Chem. Eng. Technol.*, **13**, 229-237.
- Hendriksen, B.A., D.J.W. Grant, P. Meenan, and D.A. Green (1998). Crystallization of paracetamol (acetaminophen) in the presence of structurally related substances. *J. Crystal Growth*, **183**, 629-640.
- Hukkanen, E.J., and R.D. Braatz (2002). Measurement of particle size distribution in suspension polymerization using in situ laser backscattering. Department of Chemical and Biomolecular Engineering, University of Illinois at Urbana-Champaign, technical report.
- Kim, K.-J., and A. Mersmann (2001). Estimation of metastable zone width in different nucleation processes. *Chem. Eng. Sci.*, **56**, 2315-2324.
- Lewiner, F., G. Fevotte, J.P. Klein, and F. Puel (2001). Improving batch cooling seeded crystallization of an organic weed-killer using on-line ATR FTIR measurement of supersaturation. *J. Crystal Growth*, **226**, 348-362.
- Ma, D.L., and R.D. Braatz (2003). Robust identification and control of batch processes. *Comp. & Chem. Eng.*, in press.
- Ma, D.L., S.H. Chung, and R.D. Braatz (1999). Worst-case performance analysis of optimal batch control trajectories. *AIChE J.*, **45**, 1469-1476.
- Miller, S.M., and J.B. Rawlings (1994). Model identification and control strategies for batch cooling crystallizers. *AIChE J.*, **40**, 1312-1327.
- Mullin, J.W. (1993). *Crystallization*. 3rd edition, Butterworth-Heinemann, London.
- Nagy, Z.K., and R.D. Braatz (2002). Comparison between open-loop and closed-loop robust optimal control of batch processes using distributional worst-case analysis. *J. Proc. Cont.*, submitted.
- Nagy, Z.K., M. Fujiwara, and R.D. Braatz (2002). Determination of kinetic parameters for batch pharmaceutical crystallization using metastable zone experiments. Department of Chemical and Biomolecular Engineering, University of Illinois at Urbana-Champaign, technical report.
- Rawlings, J.B., S.M. Miller, and W.R. Witkowski (1993). Model identification and control of solution crystallization processes: A review. *Ind. Eng. Chem. Res.*, **32**, 1275-1296.
- Srinivasan, B., D. Bonvin, E. Visser, and S. Palanki (2003). Dynamic optimization of batch processes – II. Role of measurements in handling uncertainty, *Comp. & Chem. Eng.*, **27**, 27-44.
- Terwiesc, P., M. Agarwal, and D.W.T. Rippin (1994). Batch unit optimization with imperfect modeling: a survey. *J. Proc. Cont.*, **4**, 238-258.
- Togkalidou, T., M. Fujiwara, S. Patel, and R.D. Braatz (2001). Solute concentration prediction using chemometrics and ATR-FTIR spectroscopy. *J. Crystal Growth*, **231**, 534-543.